

## ON ACCELERATION STATISTICS IN TURBULENT STRATIFIED SHEAR FLOWS

**Frank G. Jacobitz**

Mechanical Engineering Department  
Shiley-Marcos School of Engineering  
University of San Diego  
5998 Alcalá Park, San Diego, CA 92110, USA  
jacobitz@sandiego.edu

**Kai Schneider**

M2P2-CNRS  
Aix-Marseille Université  
38 rue Joliot-Curie,  
13451 Marseille Cedex 20, France  
kschneid@cmi.univ-mrs.fr

**Marie Farge**

LMD-IPSL-CNRS  
Ecole Normale Supérieure  
24 rue Lhomond, 75231 Paris Cedex 5, France  
farge@lmd.ens.fr

### ABSTRACT

The Lagrangian and Eulerian acceleration statistics in homogeneous turbulence with uniform shear and stable stratification are studied using direct numerical simulations. The Richardson number is varied from  $Ri = 0$ , corresponding to unstratified shear flow, to  $Ri = 1$ , corresponding to strongly stratified shear flow. The probability density functions (pdfs) of both Lagrangian and Eulerian accelerations show a strong and similar influence on the Richardson number and extreme values for Eulerian acceleration are stronger than those observed for the Lagrangian acceleration. A consideration of the terms in the Navier-Stokes equation shows that the Lagrangian acceleration is mainly determined by the pressure-gradient, while the Eulerian acceleration is dominated by the nonlinear term. Similarly, the Eulerian time-rate of change of fluctuating density is observed to have larger extreme values than that of the Lagrangian time-rate of change due to the nonlinear term in the advection-diffusion equation for fluctuating density. Hence, the time-rate of change of fluctuating density obtained at a fixed location by an Eulerian observer is mainly due to advection of fluctuating density through this location, while the time-rate of change of fluctuating density following a fluid particle is substantially smaller, and due to production and dissipation of fluctuating density.

### INTRODUCTION

An understanding of the Lagrangian acceleration properties of a fluid particle in turbulent flows is of fundamental importance. After early work by Heisenberg (1948) and Yaglom (1949), recent studies range from theoretical investigations (e.g. Tsinober, 2001) to applications such as the modeling of particle dispersion (e.g. Pope, 1994). This work is carried out using both experimental (e.g. La Porta *et al.*, 2001) as well as computational (e.g. Yeung, 2002; Toschi & Bodenschatz, 2009) approaches.

The majority of previous investigations focused on Lagrangian properties of isotropic turbulence. The Lagrangian

acceleration was found to be strongly intermittent and heavy tails were observed in its pdf. For example, extreme values as high as 1,500 times the acceleration of gravity were observed for the Lagrangian acceleration of fluid particles (La Porta *et al.*, 2001) and numerical simulations confirmed these results (Toschi & Bodenschatz, 2009).

Many applications of Lagrangian dynamics target the transport and mixing of natural and anthropogenic substances in the geophysical environment. Such flows are often characterized by the presence of shear and stratification. Homogeneous turbulent stratified shear flow with constant vertical stratification rate  $S_\rho = \partial\rho/\partial y$  and constant vertical shear rate  $S = \partial U/\partial y$  represents the simplest flow configuration in order to study the competing effects of shear and stratification. This flow has been investigated extensively in the past: Experimental studies include Komori *et al.* (1983), Rohr *et al.* (1988), Piccirillo & Van Atta (1997), and Keller & Van Atta (2000). Numerical simulations include the work by Gerz *et al.* (1989), Holt *et al.* (1992), Jacobitz *et al.* (1997), and Jacobitz (2002).

The goal of this work is to investigate the acceleration statistics in turbulent stratified shear flows using direct numerical simulations. In the following, the numerical approach taken is introduced first. Then, the Richardson number dependence of the Lagrangian and Eulerian acceleration pdfs are presented, followed by a discussion of the corresponding Lagrangian and Eulerian time-rate of change pdfs for the density field.

### APPROACH

The mean flow considered in this study has a constant vertical shear rate  $S$  and a constant vertical stratification rate  $S_\rho$ :

$$U = Sy, \quad V = W = 0, \quad \rho = \rho_0 + S_\rho y \quad (1)$$

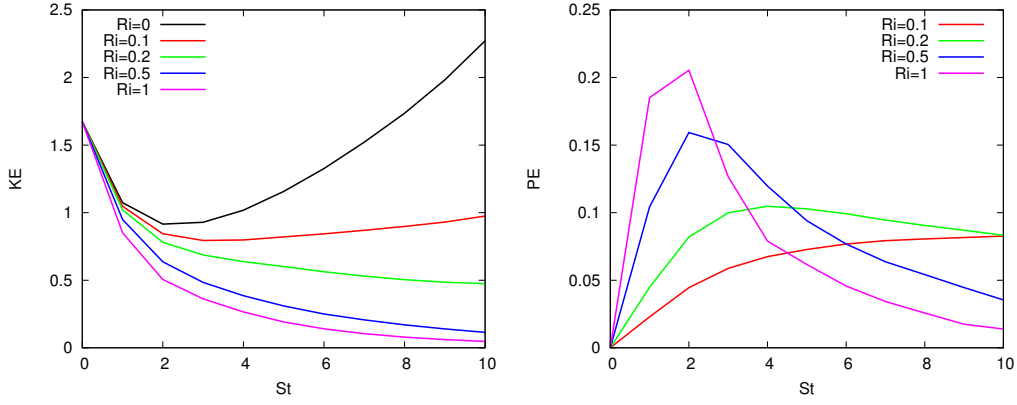


Figure 1. Evolution of the turbulent kinetic energy (left) and potential energy (right).

This study is based on the incompressible Navier-Stokes equations for the fluctuating velocity and an advection-diffusion equation for the fluctuating density:

$$\nabla \cdot \mathbf{u} = 0 \quad (2)$$

$$\begin{aligned} \frac{\partial \mathbf{u}}{\partial t} + \mathbf{u} \cdot \nabla \mathbf{u} + S_y \frac{\partial \mathbf{u}}{\partial x} + S_v \mathbf{e}_x \\ = -\frac{1}{\rho_0} \nabla p - \frac{g}{\rho_0} \rho \mathbf{e}_y + \nu \nabla^2 \mathbf{u} \end{aligned} \quad (3)$$

$$\frac{\partial \rho}{\partial t} + \mathbf{u} \cdot \nabla \rho + S_\rho v = \alpha \nabla^2 \rho \quad (4)$$

Here,  $\mathbf{u}$  is the fluctuating velocity,  $p$  the fluctuating pressure,  $\rho$  the fluctuating density,  $\nu$  the viscosity, and  $\alpha$  the scalar diffusion. The equations of motion are transformed into a frame of reference moving with the mean velocity (Rogallo, 1981). This transformation enables the application of periodic boundary conditions for the fluctuating components of velocity and a spectral collocation method is used for the spatial discretization. The solution is advanced in time with a fourth-order Runge-Kutta scheme.

The simulations are performed on a parallel computer using  $256 \times 256 \times 256$  grid points. Both the mean shear rate  $S = \partial U / \partial y$  and the mean stratification rate  $S_\rho = \partial \rho / \partial y$  are constant. The primary non-dimensional parameter, the Richardson number  $Ri = N^2 / S^2$ , where  $N$  is the Brunt-Väisälä frequency with  $N^2 = -g / \rho_0 S_\rho$ , is varied from  $Ri = 0$ , corresponding to unstratified shear flow, to  $Ri = 1$ , corresponding to strongly stratified shear flow. The initial conditions are taken from a separate simulation of isotropic turbulence without density fluctuations, which was allowed to develop for approximately one eddy turnover time. The initial values of the Taylor-microscale Reynolds number  $Re_\lambda = 56$  and the shear number  $SK / \varepsilon = 2$  are fixed.

## RESULTS

In this section, the flow evolution, Lagrangian and Eulerian accelerations, as well as Lagrangian and Eulerian time-rates of change of the density are discussed.

## Turbulence Evolution

In order to provide a context for the present study, the energetics of the flow is briefly discussed. Details can be found in Jacobitz *et al.* (1997) and Jacobitz (2002). Figure 1 (left) shows the evolution of the turbulent kinetic energy  $K$ . As the Richardson number  $Ri$  is increased, the evolution of the turbulent kinetic energy changes from growth to decay at a critical value of  $Ri_{cr} \approx 0.15$ .

The potential energy  $K_\rho$  is defined as:

$$K_\rho = \frac{1}{2} \frac{g}{S_\rho \rho_0} \rho^2 \quad (5)$$

Figure 1 (right) shows that the potential energy initially grows due to an increasing stratification rate with increasing  $Ri$ . Eventually, however, the decay of  $K$  also affects the evolution of  $K_\rho$  for large Richardson numbers.

## Lagrangian and Eulerian Accelerations

The Lagrangian and Eulerian accelerations are defined as

$$\mathbf{a}_L = \frac{\partial \mathbf{u}}{\partial t} + \mathbf{u} \cdot \nabla \mathbf{u} \quad \text{and} \quad \mathbf{a}_E = \frac{\partial \mathbf{u}}{\partial t}, \quad (6)$$

respectively. This definition of the Lagrangian acceleration implies the perspective of an observer traveling with a fluid particle and the effects of shear and stratification are considered to be external forces. In the following, the accelerations are analyzed at time instant  $St = 5$ .

Figure 2 shows the probability distribution functions (pdfs) of the Lagrangian acceleration  $\mathbf{a}_L$  (left) and of the Eulerian acceleration  $\mathbf{a}_E$  (right). The pdfs of both accelerations have stretched-exponential shapes and they exhibit a strong and similar influence on the Richardson number  $Ri$ . Figure 3 shows the normalized pdfs of the two accelerations. For a core region of about three standard deviations, both the Lagrangian and Eulerian accelerations show approximately the same shape. The tails of the pdfs of both accelerations were observed to be heavier for smaller  $Ri$  and the extreme values of the Eulerian acceleration are above those of the Lagrangian acceleration, which is consistent with previous observations for sheared and rotating turbulence (Jacobitz *et al.*, 2013).

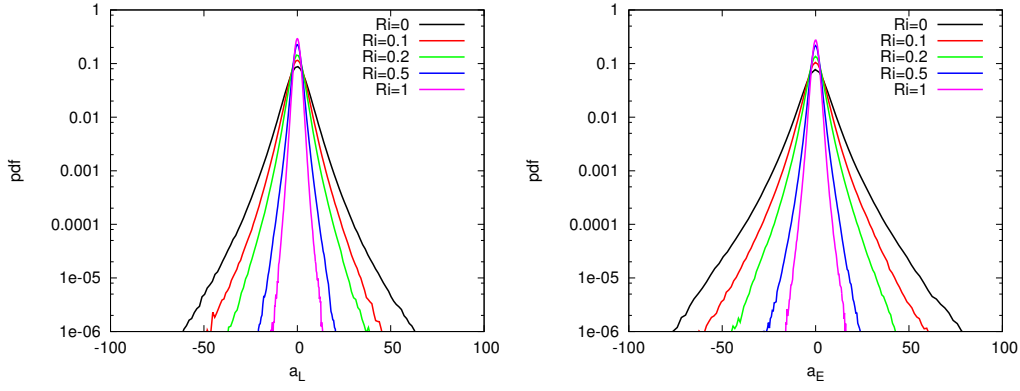


Figure 2. Pdfs of Lagrangian acceleration  $\mathbf{a}_L$  (left) and Eulerian acceleration  $\mathbf{a}_E$  (right).

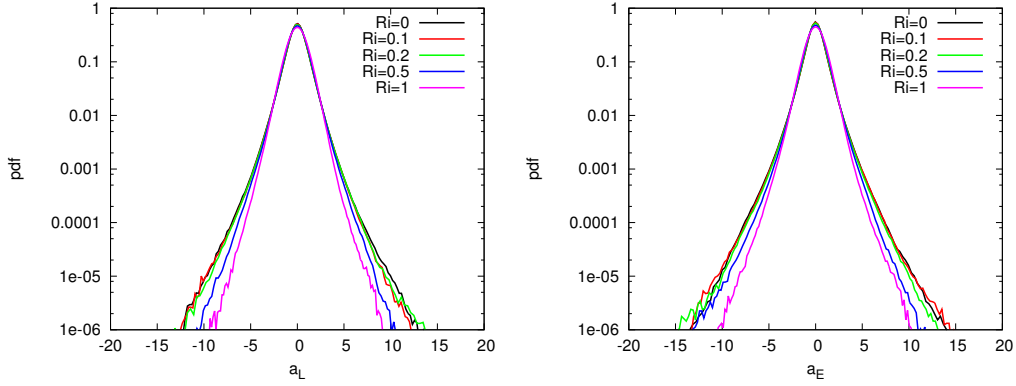


Figure 3. Normalized pdfs of Lagrangian acceleration  $\mathbf{a}_L$  (left) and Eulerian acceleration  $\mathbf{a}_E$  (right).

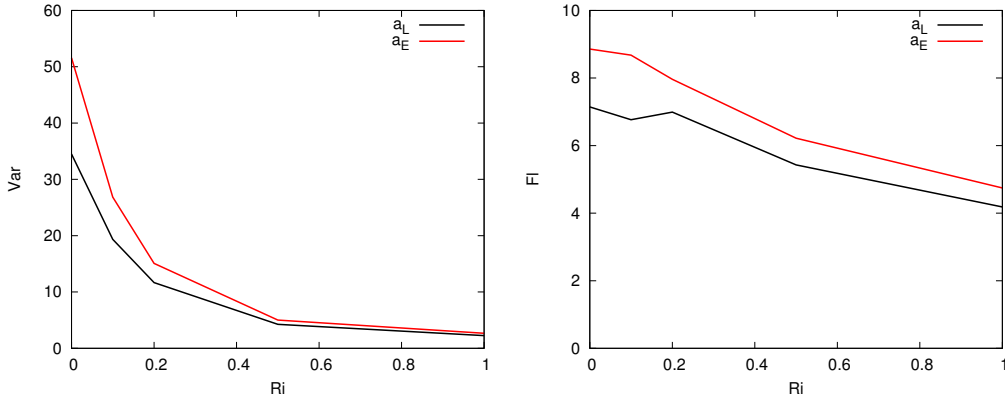


Figure 4. Variation of the variance (left) and flatness (right) of the Lagrangian and Eulerian accelerations with Richardson number  $Ri$ .

The variance of the acceleration pdfs are shown in figure 4 (left). The variance of both accelerations decrease with increasing  $Ri$  and the variance of  $\mathbf{a}_E$  remains always larger than the variance of  $\mathbf{a}_L$ . The heavier tails observed for the pdf of  $\mathbf{a}_E$  as compared to  $\mathbf{a}_L$  results in a larger flatness of the Eulerian acceleration pdf as compared to its Lagrangian counterpart. Again, both flatness values decrease with increasing  $Ri$ , indicating a decreased importance of nonlinear effects.

Figure 5 shows pdfs of the shear term (top, left), the

buoyancy term (top, right), the pressure-gradient term (bottom, left), and the nonlinear term (bottom, right) in the Navier-Stokes equations. The shear and buoyancy terms depend linearly on velocity components and density and their pdfs have hence a Gaussian shape. While the variance of the shear term pdf decreases with increasing  $Ri$ , the variance of the buoyancy term pdf increases. The pdfs of the pressure-gradient and nonlinear terms show a stretched-exponential shape due to the quadratic nature of the terms. The variances of both terms decrease with increasing  $Ri$ . For small

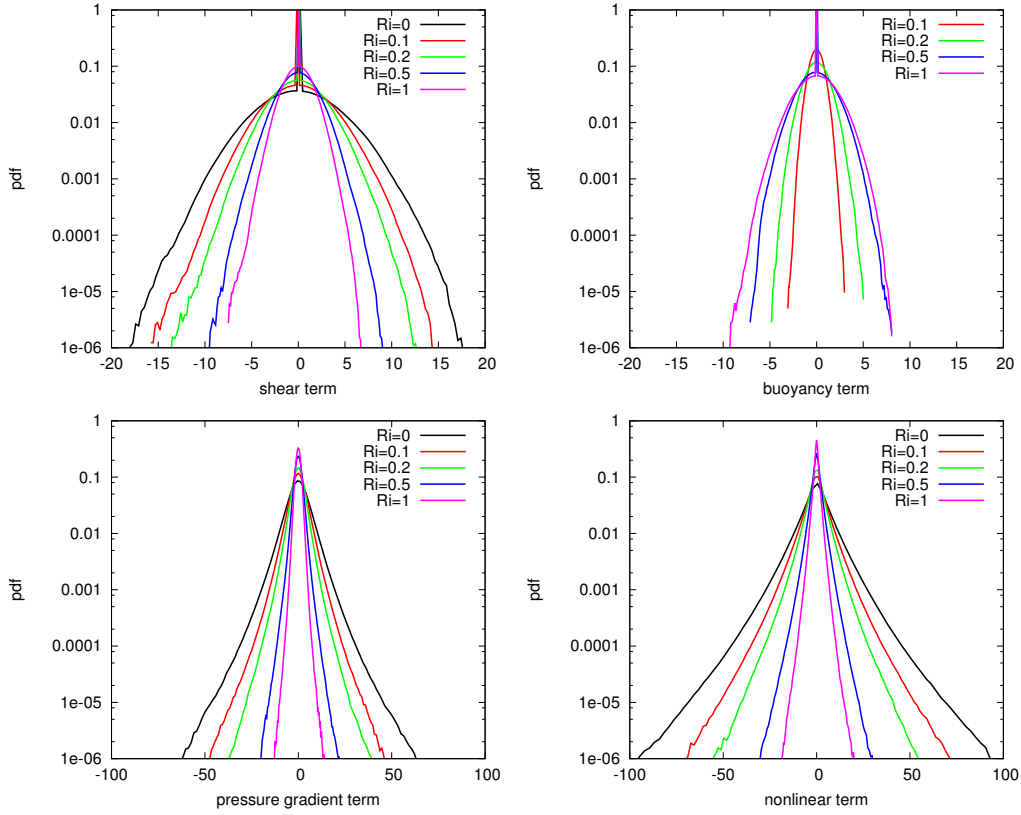


Figure 5. Pdfs of the shear (top, left), buoyancy (top, right), pressure-gradient (bottom, left), and nonlinear (bottom, right) terms in the Navier-Stokes equations.

$Ri$ , the pressure-gradient nonlinear terms clearly dominate the shear and buoyancy terms, but this dominance somewhat diminishes with increasing  $Ri$ . Hence, the pressure-gradient term is the generally dominant contribution to the Lagrangian acceleration, while the nonlinear term is important for the Eulerian acceleration.

### Lagrangian and Eulerian Time-Rates of Change

The time-rates of change of fluctuating density can also be defined using Lagrangian and Eulerian approaches as

$$s_L = \frac{\partial \rho}{\partial t} + \mathbf{u} \cdot \nabla \rho \quad \text{and} \quad s_E = \frac{\partial \rho}{\partial t}, \quad (7)$$

respectively. Figure 6 shows the pdfs of the Lagrangian time-rate of change of fluctuating density (left) and of the Eulerian time-rate of change (right). The difference in the pdfs of the time-rates of change is more pronounced than the difference obtained for the accelerations. Figure 7 shows the normalized pdfs of the two time-rates of change. While the shape of the Eulerian time-rate of change pdf is again found to be stretched-exponential, the Lagrangian time-rate of change pdf has an almost Gaussian shape. The extreme values of the Eulerian time-rate of change of fluctuating density are substantially larger than those of the Lagrangian time-rate of change.

Figure 8 (left) shows the dependence of the variance of the time-rate of change pdfs on the Richardson number  $Ri$ .

Note that for  $Ri = 0$ , the density is a passive scalar (zero gravity) with a mean gradient. For the buoyant cases with  $Ri > 0$ , the variance of both time-rates of change increases with  $Ri$  and the variance of  $s_E$  remains larger than that of  $s_L$ , consistent with the finding of the accelerations.

The flatness of the time-rates of change is shown in figure 8 (right). The flatness of  $s_E$  is always larger than that of  $s_L$ . While the flatness of  $s_E$  decreases with increasing  $Ri$ , the flatness of  $s_L$  always remains close to three, indicating a Gaussian distribution.

Figure 9 shows pdfs of the buoyancy term (left) and nonlinear term (right) in the advection-diffusion equation for fluctuating density. The buoyancy term pdf has a Gaussian shape as it is linearly related to the fluctuating density. Its variance increases with increasing  $Ri$ , because the stratification rate  $S_\rho$  increases.

The large difference observed between the Lagrangian and Eulerian time-rates of change of fluctuating density is due to the nonlinear term in the advection-diffusion equation and it is hence related to advection of fluctuating density. In other words, the time-rate of change of fluctuating density obtained at a fixed location by an Eulerian observer is mainly due to advection of density through this location, while the time-rate of change of fluctuating density observed by a Lagrangian observer following a fluid particle is substantially smaller and due to production and dissipation of fluctuating density.

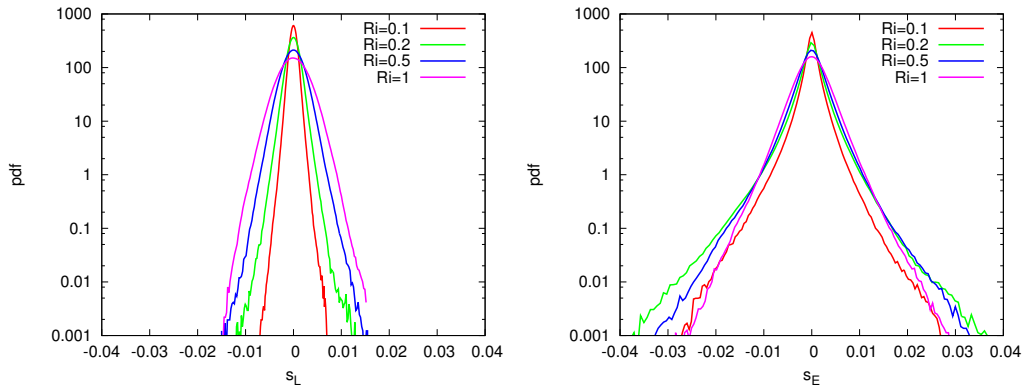


Figure 6. Pdfs of Lagrangian time-rate of change of fluctuating density  $s_L$  (left) and Eulerian time-rate of change  $s_E$  (right).

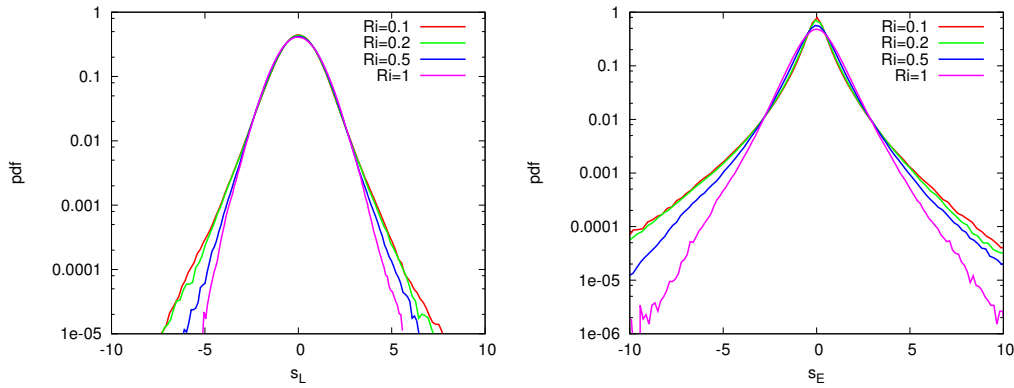


Figure 7. Normalized pdfs of Lagrangian time-rate of change of fluctuating density  $s_L$  (left) and Eulerian time-rate of change  $s_E$  (right).

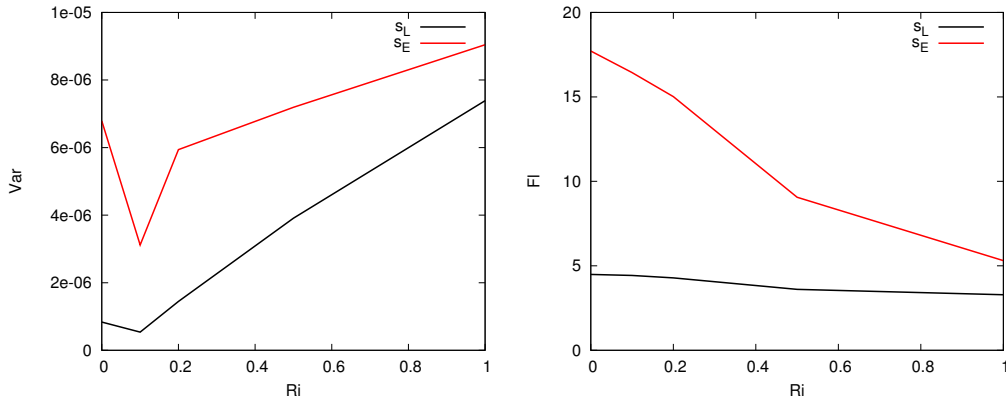


Figure 8. Variation of the variance (left) and flatness (right) of the Lagrangian and Eulerian time-rates of change with Richardson number  $Ri$ .

## CONCLUSIONS

Direct numerical simulations were performed in order to study the Lagrangian and Eulerian acceleration properties in stably stratified turbulent shear flows. With increasing Richardson number  $Ri$ , the evolution of the turbulent kinetic energy  $K$  changes from growth to decay and the variances of  $\mathbf{a}_L$  and  $\mathbf{a}_E$  decrease. The acceleration pdfs were observed to have a stretched-exponential symmetric shape and the flatness decreases with increasing  $Ri$ .

The pdfs of the pressure-gradient and nonlinear terms in the Navier-Stokes equation, which are both quadratic terms, also have stretched-exponential shapes. The Lagrangian and Eulerian accelerations are mainly determined by the pressure-gradient and the nonlinear terms, respectively. While the quadratic terms are dominant for small  $Ri$ , their dominance is somewhat diminished for large  $Ri$ . The pdfs of the shear and buoyancy terms in the Navier-Stokes equation, which are both linear terms, were observed

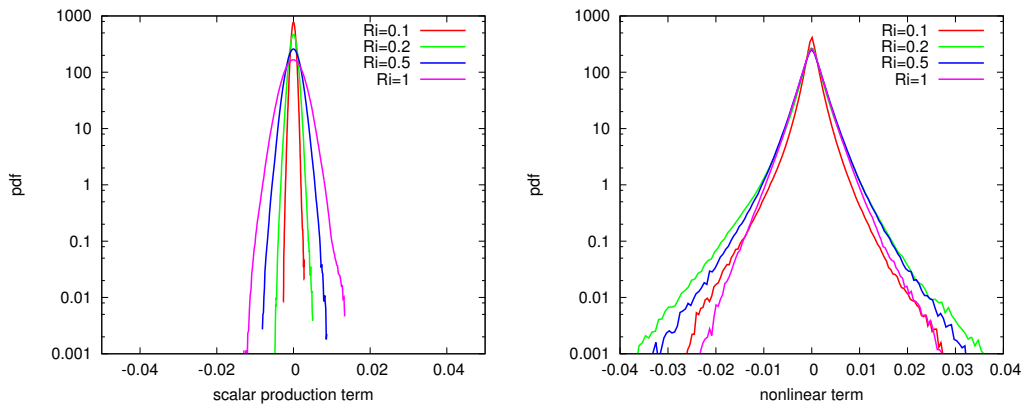


Figure 9. Pdfs of the buoyancy (left) and nonlinear (right) terms in the advection-diffusion equation for fluctuating density.

to have a Gaussian shape. While the variance of the shear term decreases with  $Ri$ , the variance of the buoyancy term increases with  $Ri$ .

In addition, the Lagrangian and Eulerian time-rates of change of density are considered. Due to a lack of a quadratic term on the right-hand-side of the advection-diffusion equation for density, the pdf of the Lagrangian time-rate of change has an almost Gaussian shape, while the pdf of the Eulerian time-rate of change was observed to have exponential to stretched-exponential shapes. The increased dominance of linear terms for strong stratification suggests that linear theory can accurately describe properties of such flows (e.g. Salhi *et al.*, 2014).

## ACKNOWLEDGMENTS

FGJ acknowledges the support from an International Opportunity Grant from the University of San Diego and the hospitality at Aix-Marseille Université. KS acknowledges financial support from the ANR, project SiCoMHD (ANR-Blanc 2011-045).

## REFERENCES

- Gerz, T., Schumann, U. & Elghobashi, S. E. 1989 Direct numerical simulation of stratified homogeneous turbulent shear flows. *J. Fluid Mech.* **200**, 563–594.
- Heisenberg, W. 1948 Zur statistischen theorie der turbulenz. *Zeitschrift für Physik* **124**, 628–657.
- Holt, S. E., Koseff, J. R. & Ferziger, J. H. 1992 A numerical study of the evolution and structure of homogeneous stably stratified sheared turbulence. *J. Fluid Mech.* **237**, 499–539.
- Jacobitz, F. G. 2002 A comparison of the turbulence evolution in a stratified fluid with vertical or horizontal shear. *J. Turbul.* **3**, 1–16.
- Jacobitz, F. G., Sarkar, S. & Van Atta, C. W. 1997 Direct numerical simulations of the turbulence evolution in a uniformly sheared and stably stratified flow. *J. Fluid Mech.* **342**, 231–261.
- Jacobitz, F. G., Schneider, K., Bos, W. J. T. & Farge, M. 2013 On multiscale acceleration statistics in rotating and sheared homogeneous turbulence. In *Proceedings of the 7th International Symposium on Turbulence and Shear Flow Phenomena*. Poitiers, France.
- Keller, K. H. & Van Atta, C. W. 2000 An experimental investigation of the vertical temperature structure of homogeneous stratified shear turbulence. *J. Fluid Mech.* **425**, 1–29.
- Komori, S., Ueda, H., Ogino, F. & Mizushima, T. 1983 Turbulence structure in stably stratified open-channel flow. *J. Fluid Mech.* **130**, 13–26.
- La Porta, A., Voth, G. A., Crawford, A. M., Alexander, J. & Bodenschatz, E. 2001 Fluid particle accelerations in fully developed turbulence. *Nature* **409**, 1017.
- Piccirillo, P. S. & Van Atta, C. W. 1997 The evolution of a uniformly sheared thermally stratified turbulent flow. *J. Fluid Mech.* **334**, 61–86.
- Pope, S. B. 1994 Lagrangian pdf methods for turbulent flows. *Annu. Rev. Fluid Mech.* **26**, 23–63.
- Rogallo, R. S. 1981 Numerical experiments in homogeneous turbulence. Technical Report TM 81315. NASA Ames Research Center, Moffett Field, CA, United States.
- Rohr, J. J., Itsweire, E. C., Helland, K. N. & Van Atta, C. W. 1988 Growth and decay of turbulence in a stably stratified shear flow. *J. Fluid Mech.* **195**, 77–111.
- Salhi, A., Jacobitz, F. G., Schneider, K. & Cambon, C. 2014 Nonlinear dynamics and anisotropic structure of rotating sheared turbulence. *Phys. Rev. E* **89**, 013020.
- Toschi, F. & Bodenschatz, E. 2009 Lagrangian properties of particles in turbulence. *Annu. Rev. Fluid Mech.* **41**, 375.
- Tsinober, A. 2001 *An informal introduction to turbulence*. Kluwer Academic Publishers.
- Yaglom, A. M. 1949 On the acceleration field in a turbulent flow. *C.R. Akad. URSS* **67**, 795–798.
- Yeung, P. K. 2002 Lagrangian investigations of turbulence. *Annu. Rev. Fluid Mech.* **34**, 115.